Green preparation and theoretical study of novel pyrimidothiazines and pyrimidooxazines using Ag/Fe₃O₄/SiO₂@MWCNTs MNCs as efficient catalyst

Atena Naeimi[1], Mahboubeh Ghasemian Dazmiri[2] and Maryam Ghazvini[3, *]

[1]Department of Chemistry, Faculty of Science, University of Jiroft, Jiroft, Iran.
[2]Facualty of Chemistry, University of Mazandaran, Babolsar, Iran.
[3]Department of Chemistry, Payame Noor University, Tehran, Iran

ARTICLE INFO

ABSTRACT

The development of Ag/Fe₃O₄/SiO₂@MWCNTs MNCs magnetic nanocomposites was done with the goal of producing novel pyrimidothiazines and pyrimidooxazines in high yields. These novel compounds were created utilizing a multicomponent reaction in aqueous media that included aldehydes, ethyl acetoacetate, urea or thiourea, electron-deficient acetylenic chemicals, and tert-butyl isocyanide. It should be noted that Petasits hybridus leaf water extract was used in these processes repeatedly to demonstrate the reusability of the nanocatalyst and was used to create the high performance nanocatalyst. The NH group, which was assessed by two processes, is what gives recently synthesized pyrimidothiazines and pyrimidooxazines their antioxidant properties. Additionally, the antibacterial activity of newly created pyrimidothiazines and pyrimidooxazines was assessed using a disk distribution procedure with two different types of Gram-negative bacteria and Gram-positive bacteria, demonstrating that using these compounds prevented the growth of bacteria. This method is used to make pyrimidothiazines and pyrimidooxazines derivatives, and it offers advantages including quick reactions, high yields for the finished products, and the ability to separate catalyst and products with ease.

1. Introduction

Due to their rigidity and considerable biological characteristics, heterocyclic compounds containing spiro moiety are particularly significant.[1] Making spiro heterocyclic compounds is significant and intriguing because this structure is also shown in natural alkaloids.[2] Among organic molecules, heterocyclic compounds are well known for exhibiting a wide range of biological characteristics.[3–15] Multicomponent reactions (MCRs), which can synthesize these compounds with significant biological activity in one pot and high yields compared to reactions with multiple steps [16, 17], are one method for making heterocyclic compounds. MCRs offer some advantages over multi-step reactions, including good product efficiency, ease of deletion, atom economy, and speedy reaction times.[18–20] We must keep in mind that many MCRs require the use of a catalyst, and that a catalyst should always be employed while performing reactions. Due to their high area active surface, chemical and electrochemical permanence, and contributions to technology and applied research, transition nanostructures play a key role among catalysts.[21] Due to the huge surface area and high adsorption capacity of MWCNTs, supported nanometals and metal oxides on MWCNTs improve catalytic performance.[22] In comparison to centrifugation and filtering, the magnetic property of Fe₃O₄ magnetic nanoparticles (MNPs) can make the removal of nanocatalyst from the reaction mixture easier and faster.[23–25] To do this, a catalyst with magnetic properties was removed from the reaction mixture using an outside magnet.

Scheme 1. Preparation of new pyrimidothiazines and pyrimidooxazines **6**
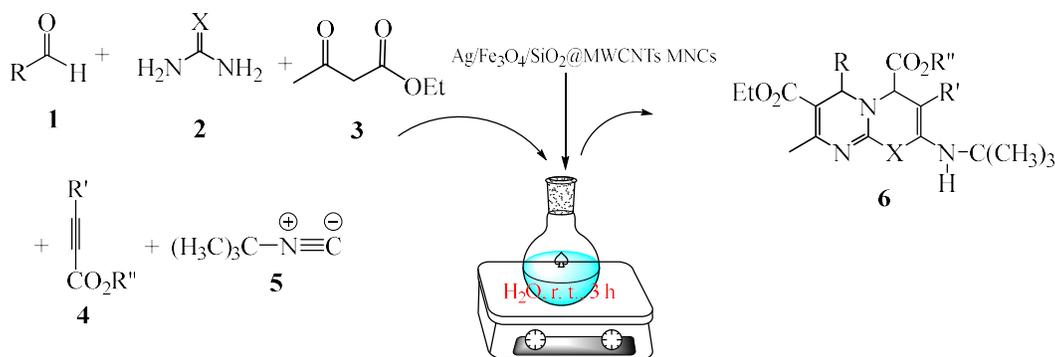
6	X	R	R'	R''	Yield of % 6
a	S	Ph	CO_2Me	Me	97
b	S	4-MeO-C_6H_4	CO_2Me	Me	98
c	S	4-Me-C_6H_4	H	Me	96
d	S	CH_3	CO_2Et	Et	90
e	O	4-NO_2-C_6H_4	CO_2Et	Et	87
f	O	4-MeO-C_6H_4	H	Me	94
g	S	CH_3CH_2	CO_2Me	Me	96
h	O	4-Me-C_6H_4	H	Et	92

In contrast to centrifuging or filtering, external magnets were utilized to remove magnetic nanocatalysts, which was a simpler and faster method. Verifying the recyclability of the nanocatalyst that is removed from the reaction mixture is crucial for nanocatalysts. The synthetic chemicals might have biologically active antibacterial and antioxidant properties. Because the organic molecules contain a molecular structure with reducing capabilities, they have antioxidant activity, which means that the harmful effects of free radicals could be reduced or even eliminated. Additionally, chemical substances with antioxidant properties may be able to prevent or cure specific diseases.[26–29] Additionally, the produced substance might have antimicrobial action, which is why the current research team looked into this aspect. Drug-resistant bacteria are harmful and can cause a variety of issues in connection with numerous infectious diseases. Finding the optimal method for resolving or decreasing this process is important for several reasons. [30-33]

We use MNCs Ag/Fe₃O₄/SiO₂@MWCNTs as organometallic catalysts to greenly synthesize new heterocyclic compounds[34-46] as we study a new method for the synthesis of pyrimidothiazines and pyrimidooxazines **6** in aqueous media at ambient temperature using MCR of aldehyde **1**, urea or thiourea **2**, acetyl ethyl acetate **3**, electron-deficient acetylenic compound **4**, tert-butyl isocyanide **5** (Scheme 1).

Experimental
General
Our research group uses starting solutions or reagents that have no chemical or physical differences. Preparation of nanocatalysts, 95% pure, 30 μm in diameter, 8 nm in diameter, from Merck. After the formation of Ag/Fe₃O₄/SiO₂@MWCNTs MNCs, the structure was analyzed by surface methods such as XRD, SEM, EDX and VSM. To obtain Ft-IR spectra from the synthesized nanocatalysts, a Shimadzu IR-460 spectrometer was used in KBr medium. Additionally, we installed a Bruker DRX-500 AVANCE spectrometer to measure 1H-NMR and ^{13}C-NMR spectra of various compounds. This spectrometer operates at 500 MHz and uses CDCl₃ as solvent and TMS as internal standard to provide characteristic results. It is noteworthy that the quality of the manufactured product with ionization energy of 70 eV was obtained using a Finnigan MAT 8430 spectrometer. Basic analysis of the resulting compounds was obtained using a Heraeus CHN-O-Rapid analyzer.

Synthesis of Ag/Fe₃O₄/SiO₂@MWCNTs MNCs [47]

For the synthesis of Ag/Fe$_3$O$_4$/SiO$_2$@MWCNTs MNCs, first the water extract of *Petasites hybridus rhizome* (5 mL) was added to the round bottom flask along with the FeCl$_2$.4H$_2$O (1.5 g), tetraethyl orthosilicate (3 mL), and then the AgNO$_3$ (1.5 g). The mixture was then heated to 100 ºC. Following the conclusion of the reaction, the mixture was mixed for a further hour. By sonicating and centrifuging the reaction mixture at 7000 rpm for roughly 30 and 10 minutes, respectively, the organic compounds that were a result of the process were removed, yielding Ag/SiO$_2$/Fe$_3$O$_4$. The *Petasites hybridus* rhizome water extract (100 mL) was added to a mixture of MWCNTs and Ag/SiO$_2$/Fe$_3$O$_4$ (0.1 g) and agitated for 1 hour at 150 ºC. The created catalyst was cleaned numerous times using a water-to-ethanol (50:50) mixture in order to separate the colloid. The catalyst was first washed with water and dried at 300 oC for 45 minutes. Following this, a high yield Ag/Fe$_3$O$_4$/SiO$_2$@MWCNTs MNCs magnetic nanocomposite was generated.

Synthesis of pyrimidothiazines and pyrimidooxazines 6a–h using a general method

After mixing the aldehydes **1** (2 mmol), urea or thiourea **2** (2 mmol), Ag/Fe$_3$O$_4$/SiO$_2$@MWCNTs MNCs (0.01 g), for 30 minutes in H$_2$O (5 mL), ethyl acetoacetate **3** (2 mmol) was added to the mixture. After 30 minutes at room temperature, a mixture of acetylenic compounds **4** (2 mmol), *tert*-butyl isocyanide **5** (2 mmol), and catalyst (0.01 g) was added to the initial mixture. These reactions were then monitored for 3 hours by thin layer chromatography (TLC). In the end, an external magnet was utilized to separate the catalyst from the reaction mixture, and the solid excess was purified using first filtering and then a second cleaning step using EtOH; Et$_2$O that resulted purified compounds **6**.

7-Ethyl 3,4-dimethyl 2-(tert-butylamino)-8-methyl-6-phenyl-4H,6H-pyrimido[2,1-b][1,3] thiazine-3,4,7-tricarboxylate (**6a**): Yellow powder, mp 123-125˚C, Yield: (96%). IR (KBr) (ν$_{max}$/cm^{-1}): 3365 (NH), 1742 (C=O), 1738 (C=O), 1698, 1587, 1484, 1295 cm^{-1}. ^{1}H NMR (500 MHz, CDCl$_3$): 1.20 (3 H, t, ^3J = 7.4 Hz, Me), 1.38 (9 H, s, Me$_3$C), 2.40 (3 H, s, Me), 3.63 (3 H, s, OMe), 3.73 (3 H, s, OMe), 4.07 (2 H, q, ^3J = 7.4 Hz, CH$_2$O), 5.54 (1 H, s, CH), 5.84 (1 H, s, CH), 7.16 (2 H, d, ^3J = 7.7 Hz, 2 CH), 7.34 (2 H, t, ^3J = 7.7 Hz, 2 CH), 7.49 (1 H, t, ^3J = 7.7 Hz, CH), 10.25 (1 H, s, NH) ppm. ^{13}C NMR (125.7 MHz, CDCl$_3$): 168.6 (C=O), 167.6 (C=O), 161.4 (C=O), 154.8, 151.6, 146.5, 137.5, 129.1, 129.0, 127.6, 105.8, 105.2, 63.0 (CH$_2$O), 60.1 (CH), 59.0 (*C*Me$_3$), 55.0 (CH), 52.7 (OMe), 51.9 (OMe), 28.9 (*CMe$_3$*), 21.4 (Me), 14.3 (Me) ppm. MS (EI, 70 eV): m/z (%): 501 (M$^+$, 15), 396 (86), 31(100). Anal. Calcd

for C$_{25}$H$_{31}$N$_3$O$_6$S (501.60): C, 59.86; H, 6.23; N, 8.38; Found: C, 59.86; H, 6.23; N, 8.38.

7-Ethyl 3,4-dimethyl 2-(tert-butylamino)-6-(4-methoxyphenyl)-8-methyl-4H,6H-pyrimido[2,1-b][1,3]thiazine-3,4,7-tricarboxylate (**6b**): Yellow powder, mp 138-140˚C, Yield: (95%). IR (KBr) (ν$_{max}$/cm^{-1}): 3467 (NH), 1739 (C=O), 1736 (C=O), 1698, 1594, 1487, 1297 cm^{-1}. ^{1}H NMR (500 MHz, CDCl$_3$): 1.21 (3 H, t, ^3J = 7.3 Hz, Me), 1.39 (9 H, s, Me$_3$C), 2.42 (3 H, s, Me), 3.64 (3 H, s, OMe), 3.75 (3 H, s, OMe), 3.78 (3 H, s, OMe), 4.08 (2 H, q, ^3J = 7.3 Hz, CH$_2$O), 5.53 (1 H, s, CH), 5.80 (1 H, s, CH), 7.23 (2 H, d, ^3J = 7.7 Hz, 2 CH), 7.34 (2 H, d, ^3J = 7.8 Hz, 2 CH), 10.28 (1 H, s, NH) ppm. ^{13}C NMR (125.7 MHz, CDCl$_3$): 168.6 (C=O), 167.6 (C=O), 161.4 (C=O), 154.8, 151.6, 146.5, 137.5, 129.1, 129.0, 127.6, 105.8, 105.2, 63.0, 60.1, 59.0, 55.0, 52.7, 51.9, 28.9, 21.4 (Me), 14.3 (Me) ppm. MS (EI, 70 eV): m/z (%): 531 (M$^+$, 15), 412 (68), 45(100). Anal. Calcd for C$_{26}$H$_{33}$N$_3$O$_7$S (531.62): C, 58.74; H, 6.26; N, 7.90; Found: C, 58.74; H, 6.26; N, 7.90.

7-Ethyl 4-methyl 2-(tert-butylamino)-8-methyl-6-(p-tolyl)-4H,6H-pyrimido[2,1-b][1,3]thiazine-4,7-dicarboxylate (**6c**): Yellow powder, mp 137-139˚C, Yield: (96%). IR (KBr) (ν$_{max}$/cm^{-1}): 3525 (NH), 1743 (C=O), 1738 (C=O), 1697, 1589, 1486, 1297 cm^{-1}. ^{1}H NMR (500 MHz, CDCl$_3$): 1.23 (3 H, t, ^3J = 7.3 Hz, Me), 1.37 (9 H, s, Me$_3$C), 2.39 (3 H, s, Me), 2.42 (3 H, s, Me), 3.73 (3 H, s, OMe), 4.07 (2 H, q, ^3J = 7.3 Hz, CH$_2$O), 5.00 (1 H, s, CH), 5.72 (1 H, s, CH), 6.12 (1 H, s, CH), 7.24 (2 H, d, ^3J = 7.8 Hz, 2 CH), 7.35 (2 H, d, ^3J = 7.8 Hz, 2 CH), 10.32 (1 H, s, NH) ppm. ^{13}C NMR (125.7 MHz, CDCl$_3$): 168.6, 167.6, 161.4, 154.8, 151.6, 146.5, 137.5, 129.1, 129.0, 127.6, 105.8, 105.2, 63.0, 60.1, 59.0, 55.0, 52.7, 51.9, 28.9, 21.4 (Me), 14.3 (Me) ppm. MS (EI, 70 eV): m/z (%): 457 (M$^+$, 10), 322 (86), 31(100). Anal. Calcd for C$_{24}$H$_{31}$N$_3$O$_4$S (457.59): C, 63.00; H, 6.83; N, 9.18; Found: C, 63.00; H, 6.83; N, 9.18.

Triethyl 2-(tert-butylamino)-6,8-dimethyl-4H,6H-pyrimido[2,1-b][1,3]thiazine-3,4,7-tricarboxylate (**6d**): Yellow powder, mp 143-145˚C, Yield: (90%). IR (KBr) (ν$_{max}$/cm^{-1}): 3457 (NH), 1742 (C=O), 1738 (C=O), 1698, 1579, 1486, 1298 cm^{-1}. ^{1}H NMR (500 MHz, CDCl$_3$): 1.15 (3 H, t, ^3J = 7.3 Hz, Me), 1.20 (3 H, t, ^3J = 7.4 Hz, Me), 1.26 (3 H, t, ^3J = 7.4 Hz, Me), 1.38 (9 H, s, Me$_3$C), 1.44 (3 H, d, ^3J = 6.8 Hz, Me), 2.37 (3 H, s, Me), 4.08 (2 H, q, ^3J = 7.4 Hz, CH$_2$O), 4.16 (2 H, q, ^3J = 7.4 Hz, CH$_2$O), 4.21 (2 H, q, ^3J = 7.3 Hz, CH$_2$O), 5.17 (1 H, q, ^3J = 7.5 Hz, CH), 5.43 (1 H, s, CH), 10.28 (1 H, s, NH) ppm. ^{13}C NMR (125.7 MHz, CDCl$_3$): 167.3, 167.2, 163.7, 156.9, 152.3, 146.4, 105.8, 105.1, 63.8,

61.4, 60.4, 60.4, 55.0, 52.4, 28.9, 21.1, 19.3, 14.3, 14.3, 14.0 ppm. MS (EI, 70 eV): m/z (%): 467 (M+, 15), 354 (74), 31(100). Anal. Calcd for $C_{22}H_{33}N_3O_6S$ (467.58): C, 56.51; H, 7.11; N, 8.99; Found: C, 56.51; H, 7.11; N, 8.99.

Triethyl 2-(tert-butylamino)-8-methyl-6-(4-nitrophenyl)-4H,6H-pyrimido[2,1-b][1,3]oxazine-3,4,7-tricarboxylate (**6e**): Yellow powder, mp 158-160°C, Yield: (87%). IR (KBr) (v_{max}/cm^{-1}): 3547 (NH), 1743 (C=O), 1739 (C=O), 1698, 1629, 1593, 1495, 1287 cm^{-1}. 1H NMR (500 MHz, CDCl$_3$): 1.16 (3 H, t, ^3J = 7.2 Hz, Me), 1.23 (3 H, t, ^3J = 7.4 Hz, Me), 1.28 (3 H, t, ^3J = 7.4 Hz, Me), 1.39 (9 H, s, Me$_3$C), 2.38 (3 H, s, Me), 4.09 (2 H, q, ^3J = 7.2 Hz, CH$_2$O), 4.14 (2 H, q, ^3J = 7.4 Hz, CH$_2$O), 4.23 (2 H, q, ^3J = 7.4 Hz, CH$_2$O), 5.12 (1 H, s, CH), 5.74 (1 H, s, CH), 7.32 (2 H, d, ^3J = 7.8 Hz, 2 CH), 8.02 (2 H, d, ^3J = 7.8 Hz, 2 CH) 10.52 (1 H, s, NH) ppm. 13C NMR (125.7 MHz, CDCl$_3$): 167.3, 167.0, 164.8, 157.6, 154.2, 148.2, 145.8, 141.9, 130.0, 124.4, 124.5, 103.7, 88.9, 61.4, 60.5, 60.4, 60.1, 55.9, 53.1, 29.2, 21.1, 14.3, 14.4, 14.0 ppm. ppm. MS (EI, 70 eV): m/z (%): 558 (M+, 10), 410 (64), 31(100). Anal. Calcd for $C_{27}H_{34}N_4O_9$ (558.59): C, 58.06; H, 6.14; N, 10.03; Found: C, 58.06; H, 6.14; N, 10.03.

7-Ethyl 4-methyl 2-(tert-butylamino)-6-(4-methoxyphenyl)-8-methyl-4H,6H-pyrimido[2,1-b][1,3]oxazine-4,7-dicarboxylate (**6f**): Yellow powder, mp 161-163°C, Yield: (94%). IR (KBr) (v_{max}/cm^{-1}): 3357 (NH), 1742 (C=O), 1738 (C=O), 1695, 1635, 1593, 1486, 1298 cm^{-1}. 1H NMR (500 MHz, CDCl$_3$): 1.18 (3 H, t, ^3J = 7.5 Hz, Me), 1.38 (9 H, s, Me$_3$C), 1.46 (3 H, d, ^3J = 7.6 Hz, Me), 3.63 (3 H, s, OMe), 3.73 (3 H, s, OMe), 4.09 (2 H, q, ^3J = 7.6 Hz, CH$_2$O), 5.18 (1 H, q, ^3J = 7.5 Hz, CH), 5.45 (1 H, s, CH), 10.28 (1 H, s, NH) ppm.13C NMR (125.7 MHz, CDCl$_3$): 167.4, 167.2, 159.5, 157.6, 147.5, 147.5, 133.3, 129.7, 114.3, 104.5, 86.5, 60.1, 55.3, 55.0, 54.4, 52.4, 51.6, 29.1, 21.1, 14.3 ppm. MS (EI, 70 eV): m/z (%): 529 (M+, 10), 380 (64), 31(100). Anal. Calcd for $C_{24}H_{31}N_3O_6$ (457.53): C, 63.00; H, 6.83; N, 9.18; Found: C, 63.00; H, 6.83; N, 9.18.

7-Ethyl 3,4-dimethyl 2-(tert-butylamino)-6-ethyl-8-methyl-4H,6H-pyrimido[2,1-b][1,3]thiazine-3,4,7-tricarboxylate (**6g**): Yellow powder, mp 176-178°C, Yield: (96%). IR (KBr) (v_{max}/cm^{-1}): 3426 (NH), 1745 (C=O), 1739 (C=O), 1699, 1637, 1594, 1488, 1297 cm^{-1}. 1H NMR (500 MHz, CDCl$_3$): 0.94 (3 H, t, ^3J = 7.3 Hz, Me), 1.21 (3 H, t, ^3J = 7.4 Hz, Me), 1.39 (9 H, s, Me$_3$C), 1.88 (2 H, m, CH$_2$), 2.13 (3H, s, CH$_3$), 3.64 (3 H, s, OMe), 3.75 (3 H, s, OMe), 4.12 (2 H, q, ^3J = 7.6 Hz, CH$_2$O), 4.72 (1 H, m, CH), 5.43 (1 H, s, CH), 10.45 (1 H, s, NH) ppm. 13C NMR (125.7 MHz, CDCl$_3$): δ 168.7, 167.4, 161.5, 154.7, 152.6, 146.4, 106.5, 106.0, 62.8,

60.3, 56.7, 55.0, 52.7, 51.9, 28.9, 27.3, 21.1, 14.3, 10. ppm. MS (EI, 70 eV): m/z (%): 453 (M+, 10), 422 (64), 31(100). Anal. Calcd for $C_{21}H_{31}N_3O_6S$ (453.55): C, 55.61; H, 6.89; N, 9.26; Found: C, 55.61; H, 6.89; N, 9.26.

Diethyl 2-(tert-butylamino)-8-methyl-6-(p-tolyl)-4H,6H-pyrimido[2,1-b][1,3]oxazine-4,7-dicarboxylate (**6h**): Yellow powder, mp 169-171°C, Yield: (92%). IR (KBr) (v_{max}/cm^{-1}): 3435 (NH), 1742 (C=O), 1738 (C=O), 1687, 1592, 1485, 1294 cm^{-1}. 1H NMR (500 MHz, CDCl$_3$): 1.21 (3 H, t, ^3J = 7.2 Hz, Me), 1.25 (3 H, t, ^3J = 7.4 Hz, Me), 1.34 (9 H, s, Me$_3$C), 2.34 (3 H, s, Me), 2.43 (3 H, s, Me), 4.10 (2 H, q, ^3J = 7.2 Hz, CH$_2$O), 4.21 (2 H, q, ^3J = 7.4 Hz, CH$_2$O), 5.06 (1 H, s, CH), 5.75 (1 H, s, CH), 5.79 (1 H, s, CH), 7.10 (2 H, d, ^3J = 7.8 Hz, 2 CH), 7.15 (2 H, d, ^3J = 7.8 Hz, 2 CH) 10.64 (1 H, s, NH) ppm. 13C NMR (125.7 MHz, CDCl$_3$): δ 167.2, 166.9, 157.6, 147.5, 147.4, 137.7, 136.4, 130.0, 128.9, 128.9, 104.5, 86.5, 60.8, 60.1, 55.2, 55.05, 51.6, 29.1, 21.1, 21.0, 14.3, 14.0 ppm. MS (EI, 70 eV): m/z (%): 455 (M+, 15), 425 (68), 31(100). Anal. Calcd for $C_{25}H_{33}N_3O_5$ (455.56): C, 65.91; H, 7.30; N, 9.22; Found: C, 65.91; H, 7.30; N, 9.22.

DPPH as reagent for evaluation of antioxidant property of pyrimidothiazines and pyrimidooxazines

By using DPPH as a radical trap, Shimada et al.'s method [48] was used to evaluate the antioxidant properties of pyrimidothiazines and pyrimidooxazines **6a–6d**. The antioxidant properties of the synthesized pyrimidothiazines and pyrimidooxazines **6a–6d** were investigated using the Shimada technique. For the purpose of examining this property, these chosen chemicals, whose concentrations ranged from 200 to 1000 ppm, were added to the same volume of a methanolic solution of DPPH (1 mmol/L). After combining pyrimidothiazines, pyrimidooxazines, and DPPH at room temperature for 30 minutes, the mixture's absorbance was measured in a dark area, yielding a value of 517 nm. When methanol (3 mL) was used as an alternative to butylated hydroxytoluene (BHT) and 2-tertbutylhydroquinone (TBHQ), the antioxidant activity of the synthesized pyrimidothiazines and pyrimidooxazines 6a–6d was evaluated. We assessed the amount of DPPH radical inhibition applying the Yen and Duh [49] equation.

FRAP process for study of Antioxidant property of pyrimidothiazines and pyrimidooxazines

The method devised by Yildirim et al. was used in the current investigation into the antioxidant properties of prepared pyrimidothiazines and pyrimidooxazines [50].

In this process, pyrimidothiazines and pyrimidooxazines **6a–d** reduced iron (III). The generated pyrimidothiazines and pyrimidooxazines solution (1 mL), ferricyanide potassium (2.6 mL), and buffer of phosphate (2.6 mL) were therefore agitated and combined at 55 oC for 35 min. After adding 2.5 mL of acid trichloroacetic to the first mixture, the latter was centrifuged for 10 minutes. $FeCl_3$ (0.6 mL), deionized water (2.6 mL), and supernatant (2.5 mL) were combined, and their absorbance at 700 nm was measured. It is important to remember that the high levels of reducing are what cause the high absorbance. For giving good results, the experiments were performed three times.

Study of pyrimidothiazines and pyrimidooxazines as antibacterial agents

The examination of antibacterial properties using two different types of Gram-positive and Gram-negative bacteria was another area of study. The Persian Type Culture Collection (PTCC), Tehran, Iran, provided these bacteria for use in the disk diffusion procedure. The two types of bacteria were cultured for 16 to 24 hours at 37 °C to provide the identical McFarland Standard No. 0.5 for this operation. We used the standards of streptomycin and gentamicin to kill two different types of bacteria. Using a sterile swab used for culturing, the bacteria were produced (1.52 108 CFU/mL) in accordance with McFarland Standard No. 0.5 and Mueller Hinton agar. 25 g/ml of pyrimidothiazines and pyrimidooxazines were then poured on sterile blank disks and placed in an incubator for 24 hours at 37 °C for measuring diameter of these compounds. We then made a comparison between it and inhibition zone for confirmation of antibacterial activity of supplied derivatives of these compounds. The plates were placed, measured and compared with Streptomycin and Gentamicin.

Theoretical calculation

In this investigation, theoretical calculations were performed using the Gaussian 09 program to better comprehend the operation and effectiveness of the starting materials.[51] The density functional theory DFT/B3LYP approach [52-53] was employed to analyze the electronic structure and geometries, compute Mulliken atomic charges, and determine the vibrational frequencies of the synthesized chemical. The DFT approach with a 6-311++G** basis set for all atoms was chosen due to exceptional cooperation between a calculation time and an electronic correlation report. Using the Multiwfn 3.7 algorithm [54] and equations (1)

through (6) pertaining to the energies of HOMO and LUMO [55], we calculated all of the descriptors. The Pulay scaled quantum mechanical force field methodology was used to build up the observed frequencies for optimal conformity between a theoretical and experimental setting.

$$I = -E_{HOMO} \qquad (1)$$
$$A = -E_{LUMO} \qquad (2)$$
$$\mu = (E_{LUMO} + E_{HOMO})/2 \qquad (3)$$
$$\eta = (E_{LUMO} - E_{HOMO})/2 \qquad (4)$$
$$S = 1/\eta \qquad (5)$$
$$\omega = \mu^2/2\eta \qquad (6)$$

Results and discussion

Selecting the reaction's ideal states is a crucial step in the synthesis of organic compounds. To that end, a model reaction was initially mixed, using the following beginning ingredients: 4-benzaldehyde **1a**, thiourea **2a**, ethyl acetoacetate **3**, dimethyl acetylenedicarboxylate **4a**, and tert-butyl isocyanide **5** (Table 1). The model reaction was conducted for 12 hours without a catalyst and no product was found during that time, demonstrating the necessity of a catalyst for these reactions (entry 1, Table 1). Another factor for optimization is reaction temperature, thus we raised it to 100 oC for that reason; however, the yield of product **6a** did not change noticeably (entry 2, Table 1). In order to optimize the catalyst condition and produce compounds 6a in adequate yields, metal oxide nanoparticles, such as Fe_3O_4-MNPs (0.02 g), were added to the reaction mixture (entry 4, Table 1). To select the best catalyst for the reaction, we tested a range of catalysts, such as ZnO-NPs, Fe_3O_4 MNPs, Et_3N, SiO_2-NPs, Fe_3O_4/SiO_2, Fe_3O_4/MWCNT, and Ag/Fe_3O_4@MWCNTs MNCs. The results, which are displayed in Table 1, show that the most effective catalyst for completing the model reaction is Ag/Fe_3O_4@MWCNTs MNCs (0.02 g). 0.02 g of catalyst was sufficient to make 6a with a good yield (entry 10, Table 1). A rise in catalyst concentrations above 0.02 g did not yield any appreciable change in product yield.

One of the best ways to separate catalyst quickly is to magnetize the catalyst with Fe_3O_4 that has been taken out of the reaction mixture and placed on an external magnet. Another essential component for conducting reactions and obtaining high product yields is a solvent. Table 2 indicates that the optimal solvent for conducting the sample reaction is water.

When using nanocatalysts, the catalyst's capacity to be recycled is essential. As a result, the nanocatalyst was separated, cleaned, and dried at the end of the reaction in order to employ it in another reaction that was exactly

Table 1. The synthesis of pyrimidothiazines **6a**

Entry	Catalyst	Temp.(°C)	Catalyst (g)	Time (h)	Yield%[a]
1	none	r.t.	-	12	-
2	none	80	-	8	-
3	none	90	-	8	-
4	Fe_3O_4	r.t.	0.01	6	48
5	Ag/Fe_3O_4	r.t.	0.01	5	56
6	ZnO-NPs	r.t.	0.015	3	45
7	SiO_2-NPs	r.t.	0.02	3	52
8	Fe_3O_4/SiO_2	r.t.	0.02	3	65
9	**Ag/Fe₃O₄@MWCNTs**	**r.t.**	**0.02**	**3**	**97**
10	Ag/Fe_3O_4@MWCNTs	r.t.	0.025	3	97
11	Et_3N	r.t.	0.02	6	40
12	MWCNTs	r.t.	0.02	8	32
13	Ag	r.t.	0.02	5	58
14	Fe_3O_4/MWCNT NPs	r.t.	0.02	3	52

Table 2. Determination the best solvent in creation of **6a**

Entry	Solvent	Time (h)	Yield%[a]
1	EtOH	15	None
2	CH_2Cl_2	8	58
3	$CHCl_3$	5	62
4	**H₂O**	**3**	**97**
5	Solvent-free	8	48
6	DMF	12	----
7	toluene	12	74

Table 3. Reusability of nanocatalyst for synthesis of pyrimidothiazines **6a**

| Run	% Yield[a]
1	97
2	97
3	92
4	90
5	85

the same. In this investigation, the catalyst was used four times to prepare pyrimidothiazines **6a**. Table 3's results suggest that there would be no loss of activity after using the catalyst four times.

Following product purification, ^{1}H NMR, ^{13}C NMR, IR, and mass spectroscopy were used to determine the structural characteristics of the produced pyrimidothiazines and pyrimidooxazines 6. Given that all synthetic compounds have comparable functional groups, the structure of compound 6a was examined in this section as an example. One singlet at 1.38 ppm for methyl protons, three singlets at 2.40, 3.63, and 3.73 ppm for one methyl and two methoxy protons, and one singlet at 10.25 ppm for NH proton with signals for aromatic moiety can all be found in the 1H NMR spectra of compound **6a.** Three signals for the carbonyl group were visible in the 13C NMR spectra of

compound **6a** at 168.7, 167.7, and 161.5 ppm. Additionally, compound 6a's IR spectra was provided in order to establish the presence of carbonyl groups in the compound's composition. All phases of the production of pyrimidothiazines and pyrimidooxazines 6 were not described or provided with any information; nevertheless, Scheme 2 provides an explanation of the suggested mechanism of these reactions. Aldehyde 1 first reacts with thiourea or urea 2 in the presence of a nanocatalyst, generating intermediate 7 through the elimination of water. At room temperature, in the presence of Ag/Fe3O4/SiO2@MWCNTs MNCs, ethyl acetoacetate 3 reacts with intermediate 7, resulting in the production of intermediate 10 through intermolecular cyclization. Activated acetylenic esters **4** and isocyanide **5** react together for production of intermediate **11** which in the presence of catalyst react with intermediate **10** and by intermolecular cyclization prepared compounds **6**.

These reactions need the use of nanocatalysts and cannot be carried out without a catalyst. Ag/Fe₃O₄/SiO₂@MWCNTs MNCs were supplied thanks to the use of Petasites hybridus rhizome water extract, and scanning electron microscopy (SEM) was used to check the structure of the constructed catalyst. We used the image to look into and verify the skeleton of the organometallic nanocomposite. SEM analysis can be used to investigate particle volume, surface homogeny, and morphology. Magnetic nanocomposites made of Ag/Fe₃O₄/SiO₂@MWCNTs MNCs are shown in Figure 1 using SEM images. Ag/Fe₃O₄/SiO₂@MWCNTs MNCs have a spherical configuration with the nanoparticles arranged next to one another in good order, according to the FE-SEM pictures.
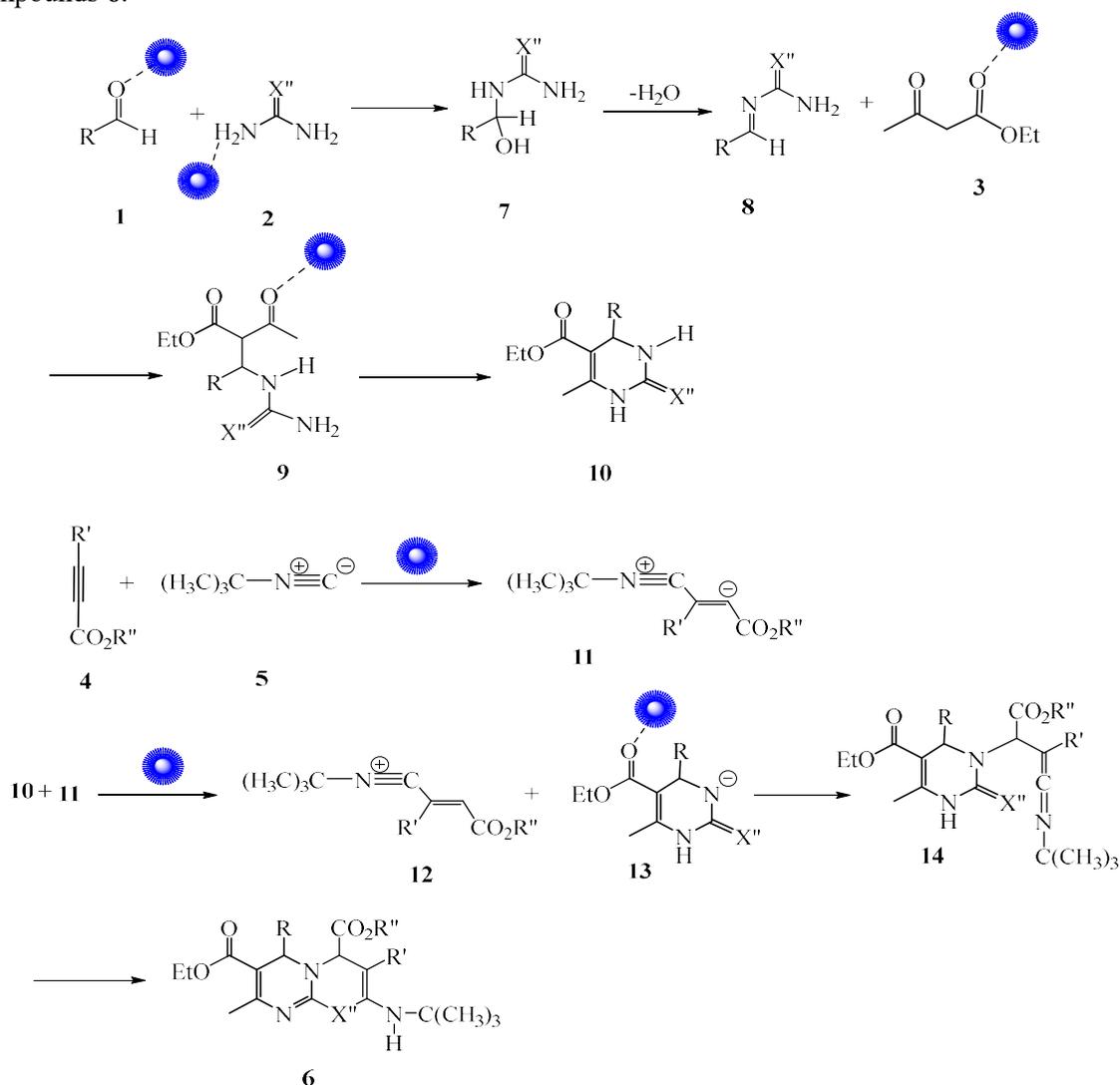
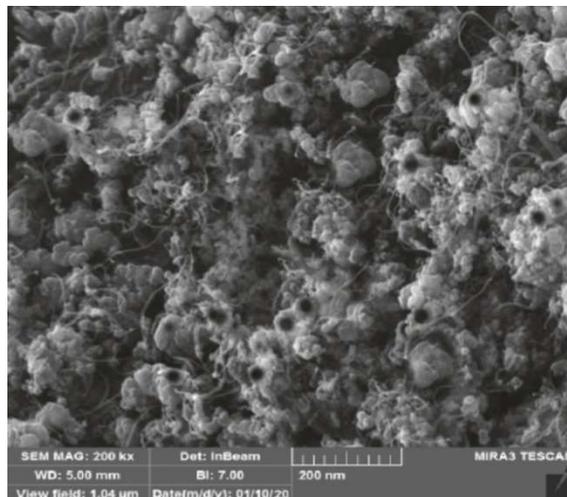**Scheme 2.** The process for the preparation of **6**

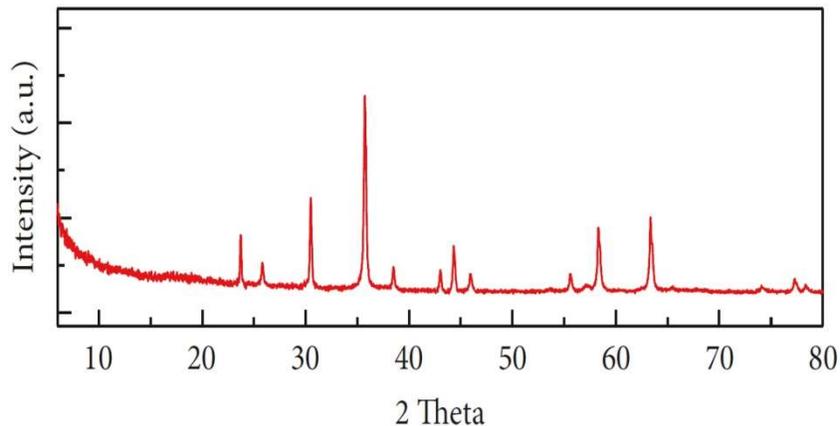**Fig. 1.** The scanning electron microscopy image of Ag/Fe$_3$O$_4$/SiO$_2$@MWCNTs MNCs

Fig. 2. X-ray diffraction spectra of Ag/Fe$_3$O$_4$/SiO$_2$@MWCNTs MNCs

Figure 2 displays the XRD analysis of the Ag/Fe$_3$O$_4$/SiO$_2$@MWCNTs MNCs. The diffraction peaks at 2 = 35.0°, 44.0°, 57.2°, and 63.0° in the XRD pattern for the synthesized Ag/Fe$_3$O$_4$/SiO$_2$@MWCNTs MNCs (Figure 2) suggest the presence of Fe3O4 MNPs (JCPDS No. 19-629). The face-centered cubic lattice of metallic Ag (JCPDS file no. 04-0783) has peaks at 2=38.3 and 46.2° planes that can suggest the presence of Ag NPs in the composites. The characteristic peak of MWNTs (JCPDS No. 41-1487) was detected as a broad crystalline peak of MWNTs between 26.0º and 43.5º. The average crystallite size of the Ag/Fe$_3$O$_4$/SiO$_2$@MWCNTs MNCs was approximately estimated 33.4 nm by Debye-Scherrer equation.
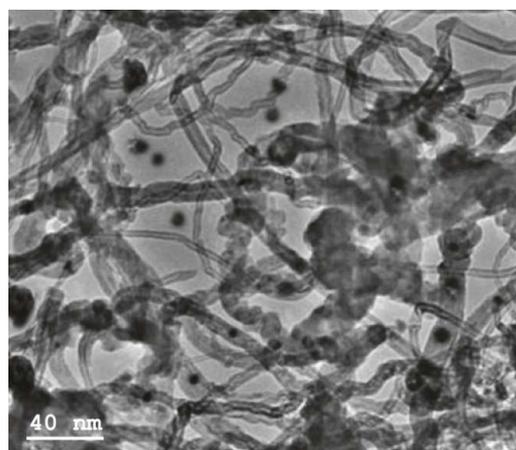

Figure 3. TEM image of the Ag/Fe$_3$O$_4$/SiO$_2$@MWCNTs

The samples were examined by TEM, as shown in Figure 3, to further study the morphology of the Ag/Fe$_3$O$_4$/SiO$_2$@MWCNTs MNCs. Ag/Fe$_3$O$_4$/SiO$_2$@MWCNTs' elemental composition was examined using the Energy Dispersive X-ray Spectroscopy (EDS) spectrum. Ag/Fe$_3$O$_4$/SiO$_2$@MWCNTs was shown to include oxygen, C, Si, Ag, and Fe (Figure 4).
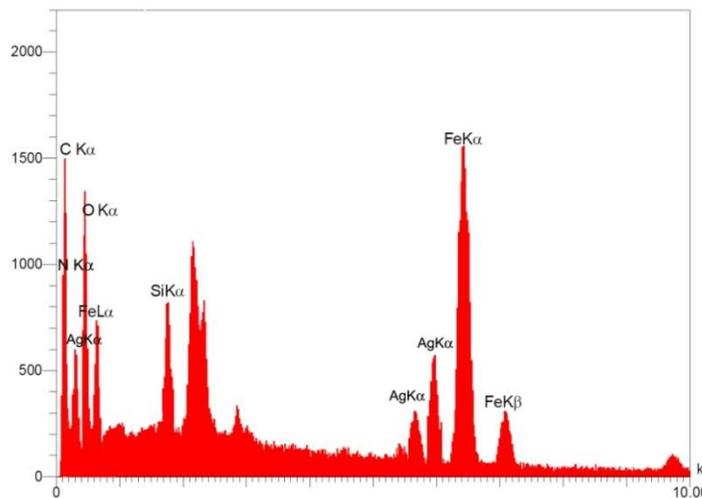

Figure 4. EDX image of Ag/Fe$_3$O$_4$/SiO$_2$@MWCNTs

The saturation magnetization (Ms) values of pure Fe$_3$O$_4$ MNPs and magnetic Ag/Fe$_3$O$_4$/SiO$_2$@MWCNT MNPs are displayed in Figure 5. Each sample showed characteristic superparamagnetic properties, with very little coercivity and remanence. The Ms of the Ag/Fe$_3$O$_4$/SiO$_2$@MWCNT (19.3 emu/g) is suppressed when compared to the pure Fe3O4 NPs (52.3 emu/g), as Figure 5 illustrates.
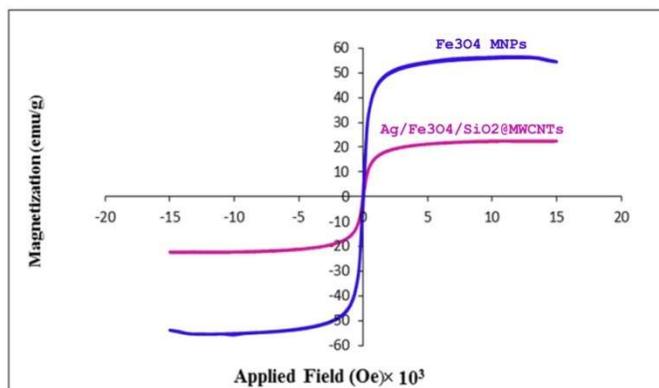

Figure 5. VSM analysis of the green Ag/Fe$_3$O$_4$/SiO$_2$@MWCNTs

Antioxidant ability Consideration of synthesized pyrimidothiazines and pyrimidooxazines by DPPH

Because synthetic molecules have a significant nucleus and NH group, the pyrimidothiazines and pyrimidooxazines produced may have antioxidant properties. DPPH was employed as a radical to demonstrate that this objective was accomplished. By using hydrogen or electron capture by free radical of DPPH, the experiment of trapping this radical is employed to ascertain the biological qualities of pyrimidothiazines and pyrimidooxazines, food, and biological structures. [56, 57] In the present investigation, it would validate the antioxidant property of the produced pyrimidothiazines and pyrimidooxazines **6a–6d** if the hydrogen or electron was taken up by DPPH free radical. Furthermore, there is a clear correlation between the percentage of produced compounds that have hydrogen or electrons adsorbed by DPPH free radicals and the level of antioxidant activity of such compounds. The DPPH radical adsorbed the electron or hydrogen from pyrimidothiazines and pyrimidooxazines **6a–6d**, confirming their antioxidant properties and causing the absorbace of DPPH to drop to 517 nm. Now, BHT and TBHQ, two common antioxidants with varying concentrations, were used to compare the antioxidant properties of pyrimidothiazines and pyrimidooxazines derivatives **6a–6d**. On the whole, the order of antioxidant ability of pyrimidothiazines and pyrimidooxazines derivatives **6a-6d** was attained as TBHQ≈BHT >**6c** > **6a** > **6b** > **6d** (Figure 6).

Determination of antioxidant ability of pyrimidothiazines and pyrimidooxazines via Fe^{3+} reducing procedure

The order of the reduced ferric ions Fe^{3+}/ferricyanide and Fe^{2+}/ferrous at 700 nm was determined by the antioxidant activity of the produced pyrimidothiazines and pyrimidooxazines **6a–6d** (Figure 7). Among the pyrimidothiazines and pyrimidooxazines tested, compound **6c** shown good reducing ability. As a result, pyrimidothiazines and pyrimidooxazines' potential to reduce emerged in the following order: **6c>6a>6b>6d**, TBHQ>BHT>.

Antibacterial activity evaluation of synthesized pyrimidothiazines and pyrimidooxazines

Synthesized pyrimidothiazines and pyrimidooxazines were compared to the antibiotics streptomycin and gentamicin for their antimicrobial activity. Table 4 shows the outcomes of this experiment. Two important and effective factors on the diameter of the inhibitory zone are the type of bacteria and the concentration of pyrimidothiazines and pyrimidooxazines. The pyrimidine-2,3-dicarboxylates **6** have the greatest effect

on Escherichia coli when compared to Gram positive and negative bacteria because they have a good diameter of inhibitory zone.

Molecular geometry

The atoms of the optimized pyrimidothiazines and pyrimidooxazines are numbered and shown in Figure 8, and Table 5 lists the energy of the optimized structures for these compounds. The optimization of all

parameters, including bond lengths and bond angles, was done using the DFT approach. The bond lengths of C-H bonds in these four created compounds are computed to be 1.9 in the current study. The bond lengths of N-H bonds and the C-N bond length for four states are measured to be 1.02 and 1.30-1.34, respectively. Because the hybridized state of C4-N5 is sp, it has a significantly shorter bond length than other C-N bonds. The $C_{21}=O_{23}$, $C_8=O_{20}$, $C_{14}=O_{33}$ bond lengths
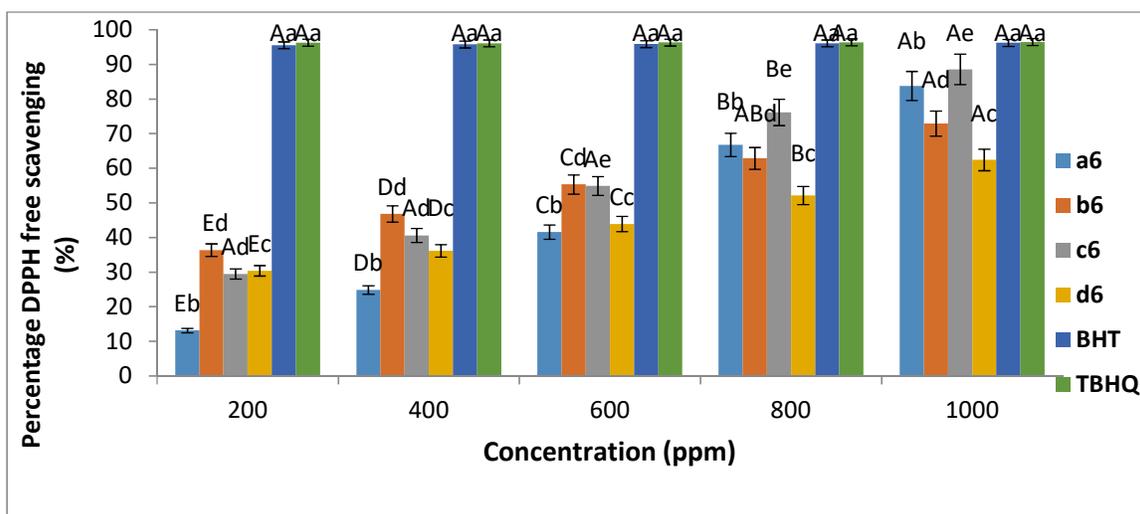

Fig. 6. Antioxidant activity of **6a-6d** compared with standards
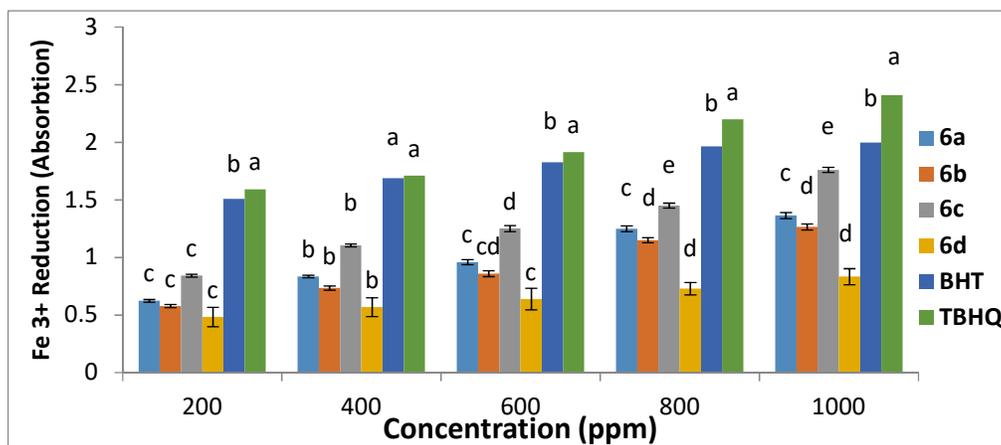

Fig. 7. The order of reducing capability of **6a-6d**

Table 4. Investigating the antibacterial activity of the synthesized pyrimidothiazines and pyrimidooxazines **6**

Compounds	Staphylococcus aureus (+)	Bacillus cereus (+)	Escherichia coli (-)	Klebsiella pneumoniae (-)
6a	18	21	23	17
6b	18	21	22	18
6c	6	9	10	10
6d	17	18	22	18
6e	7	9	8	7
6f	19	22	20	19

6g	9	9	10	8
6h	18	19	22	18
Streptomycin	21	23	23	22
Gentamicin	20	24	22	20

are calculated as 1.20-1.23 Å. The Sp^3 hybridized carbon atom bonded with C2 (sp^2) – C1 (sp^3), C7 (sp^2) – C1 (sp^3), C3 (sp^2) – C9 (sp^3) atoms, shows their bond lengths 1.50 Å and 1.52 Å respectively. The bond length of C2 (sp^2) – C8 (sp^2), C14 (sp^2) – C11 (sp^2) are 1.45 Å, which is slightly lower value, which shows its double bond character.
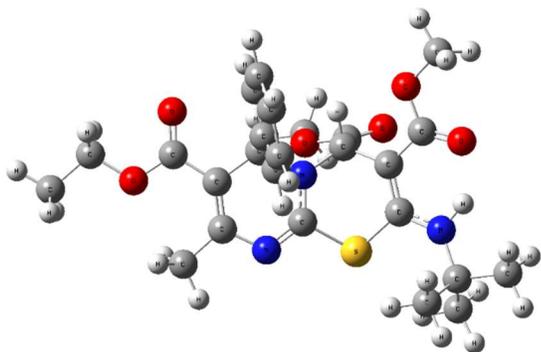

Fig. 8. The optimized molecular structure **6a**

Mulliken atomic charges

The atomic electron charge on a molecule is a key element in determining the strength of a molecule's bonds, and the Mulliken process was used to calculate the atomic charges.[58] It should be emphasized that the net atomic charge in the molecule represents the distribution of electron densities on the molecule. Table 5 and Figure **9** findings from the Mulliken atomic charge distribution demonstrate the positive or negative values of the Mulliken atomic charges on carbon atoms. In the sample optimized compound **6a-6d** as donor atoms, all hydrogen atoms have a net positive charge, whereas all oxygen and nitrogen atoms have a net negative charge. The effects of this highly electronegative atom are shown in Table 5.

Table 5. Mulliken atomic charges

	Mulliken			
	6a	**6b**	**6c**	**6d**
C1	-	-	-	-
C5	0.30625	0.30577	0.33381	0.28588
C10	-	-	-	-
C11	0.02828	0.12651	-	-
C12	0.11417	0.04049	0.07746	0.08687

HOMO-LUMO *study and Global reactivity parameters*

HOMO and LUMO are two additional crucial factors in quantum chemistry. In Figure 10, the positive and negative stages are represented by red and green colors, respectively, and these molecular orbitals provide information about the reactivity, physical, and structural features of molecules. The energy gap, which establishes the distinction between the HOMO and LUMO energies, provides information regarding the reactivity and kinetic stability of certain molecules **6a–6d**.[59] According to the molecular orbital theory used to determine the HOMO, LUMO energies and illustrate the energy gap in Table 6, the LP-LP and LP-bond pair type interactions are prevalent in the **6a-6d**. Figure 10 shows the HOMO and LUMO orbital figures together with their energies. While HOMO orbitals usually rest on phenyl groups, LUMO orbitals have a high density on carbonyl groups but are typically located near to the phenyl ring.

For **6a–6d**, the global chemical reactivity descriptors based on density functional theory were computed and are displayed in Table 7. As **6b** chemical potential (μ) values are higher than those of **6a, 6c,** and **6d**, it can be inferred that **6b** increased reactivity. Compounds **6a, 6c**, and **6d** showed increases in both chemical hardness and electrophilicity, whereas compound **6b** both showed decreases. Global chemical reactivity descriptors conducted a thoughtful analysis of the relationship between **6a-6d** structure, stability, and global chemical reactivity. The molecule is more chemically reactive, highly polarizable, and chemically soft (S) as indicated by the tiny values of η. The electron desirable of the molecule in its ground state was illustrated using the chemical potential (μ) computation. High quantities of chemical potential suggested that the molecule is more reactive and has limited stability.[60] An additional component is the global electrophilicity index (ω), which is employed in the computation of a molecule's energy stabilization in the event that an external electronic charge is acquired. Table 7 displays the antioxidant ability of compounds **6a-6d**. It indicates that compound **6b** has a high level of reactivity, and the compounds' order of antioxidant ability is **6b>6d>6c>6a**.

Molecular electrostatic potential surface
The molecular electrostatic potential is a highly useful tool for visualizing the general size, shape, and polarity of molecules as well as for locating electrophiles and nucleophiles.[61] The different intensity values determined by the molecular electrostatic potential (MEP) approach are displayed in a color spectrum for simpler comprehension of the electrostatic potential energy data. It is important to note that the link between potential growth and the color spectrum is as follows: orange (most negative), yellow (most
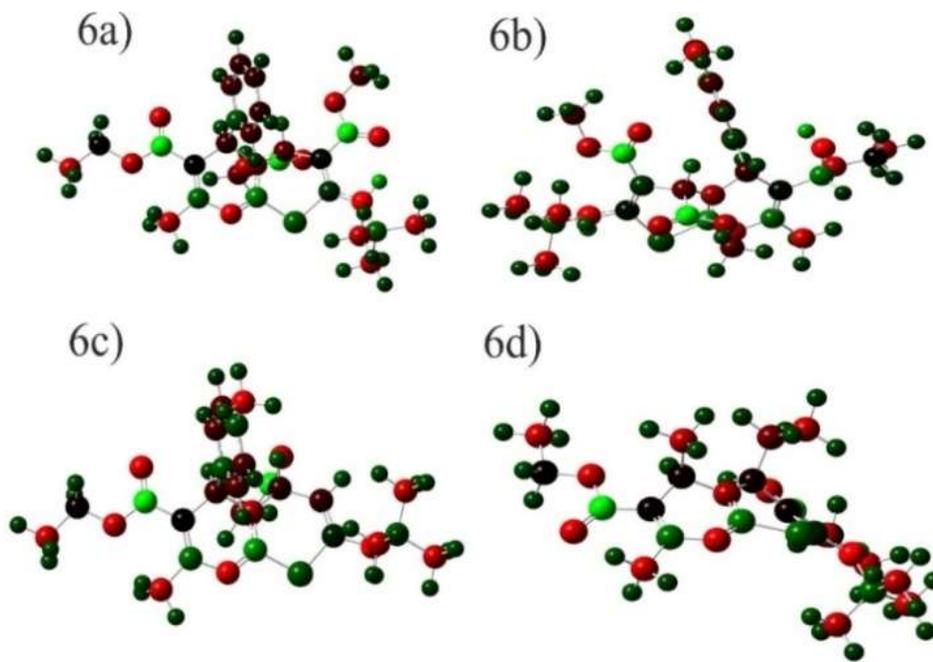

Fig. 9. The supply of Mulliken atomic charge for **6a-6d**

Table 6. Energies, band gap, dipole moment (Debye), and electronegativity

Compound	Energy(eV)	E_{LUMO}(eV)	E_{HOMO}(eV)	Eg (eV)	Gap(Ev)	D(Debye)	χ
6a	-54018.69	-0.04913	-0.20262	0.15349	4.18	0.79	3.43
6b	-	-0.04033	-0.18962	0.14929	4.06	2.66	3.13
6c	-	-0.0488	-0.20169	0.15289	4.16	1.92	3.41
6d	-	-0.04765	-0.20144	0.15379	4.18	5.43	3.39

neutral), green (most neutral), and blue (most positive). The locations of molecules that are vulnerable to electrophilic and nucleophilic assault were predicted using MEP. The electrostatic potential surface of the compounds **6a-d** can be found in Figure 11 where the color of the selected compounds **6a-d** falls in the scope of $-0.116e^{-2}$ to $+0.116e^{-2}$. Red and blue colors in the MEP structure are contributed to region with higher amounts of electron and low amount of electron, respectively. The nitrogen atoms of compounds **6a–6d** have less negative potential than the other electronegative atoms, however the regions with negative potential in the MEP are located on the oxygen and nitrogen as electronegative atoms. Therefore, the

potential locations with more positive electrostatic and negative electronegative charges are more satisfying for the compounds' suitability for nucleophilic and electrophilic performance.

Vibrational assignments
Compounds **6a-6d** has 62–72 atoms in total, and 180–210 fundamental modes of vibration. This research of the experimental FTIR spectrum was another area of concentration. The 6-311++G** basis set was used in the DFT/B3LYP approach to calculate the frequencies. An experimental factor of 0.9613 was used to scale the computed vibrational frequencies [58].
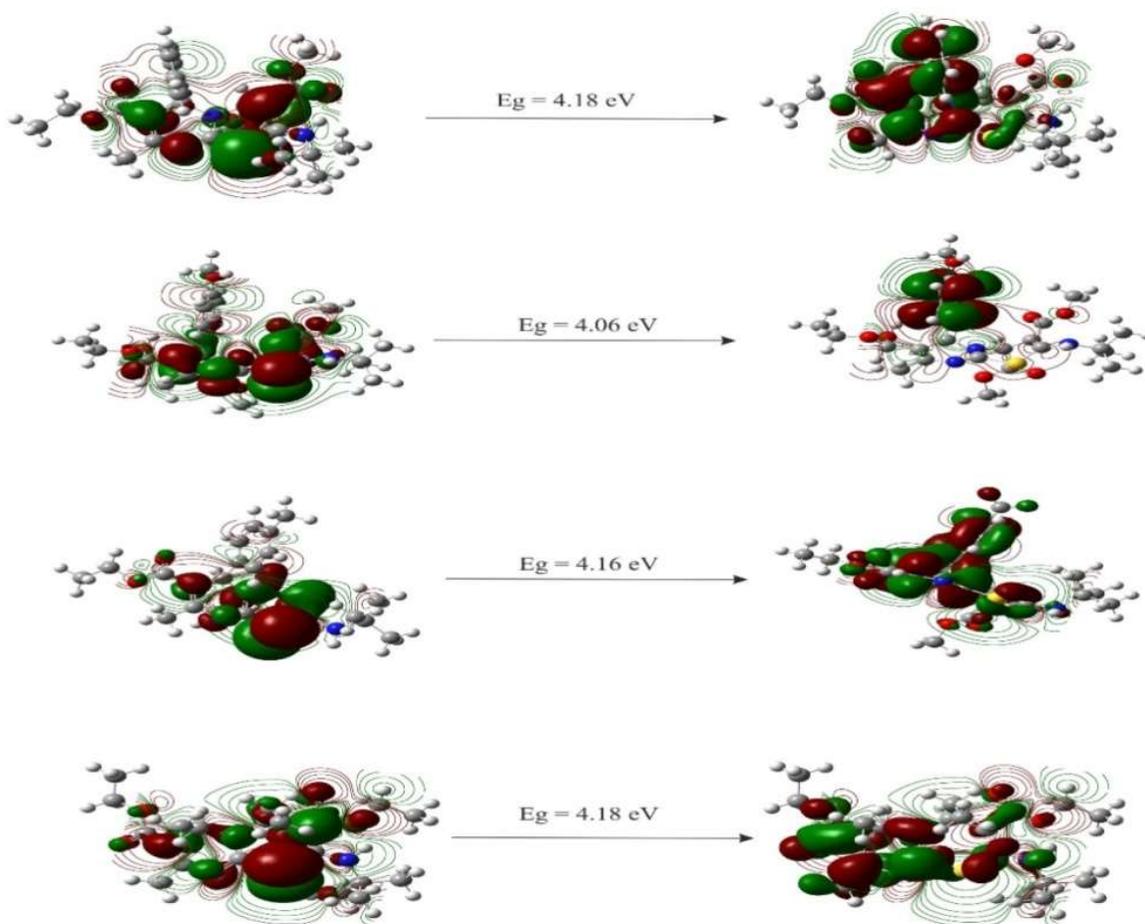
Fig. 10. Plot HOMO and LUMO orbital for compounds **6a-d**

Table 7. The outcomes of molecular parameters

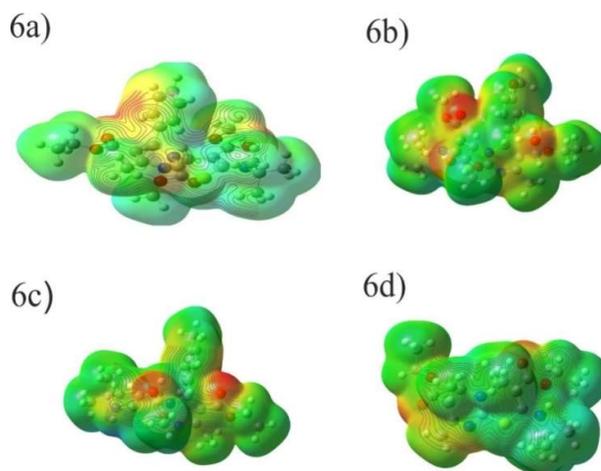| Compounds	μ	η	S	ω	I	A
6a	-3.425	2.088	0.479	11.236	4.18	5.51
6b	-3.129	2.031	0.492	9.638	4.06	5.16
6c	-3.408	2.080	0.481	11.168	4.16	5.49
6d	-3.389	2.092	0.478	10.979	4.18	5.48

Fig. 11. The electrostatic potential surface of the compounds **6a-6d**

These categories' infrared stretching frequencies altered in the same order, with C-N being 1280 cm-1 and C=N (cyanide) being 1642 cm^{-1}. In the practical technique, the stretching frequency of the carbonyl group emerged at 1767-1779 cm-1, but in the theoretical manner, it was observed at 1657-1760 cm^{-1}. The stretching frequency of aromatic C=C was found to be near together, at 1664 cm^{-1} in the experimental technique and 1642-1646 in the theoretical method.

Natural bond orbital analyses
Natural bond orbital (NBO) showed the hybridization of atomic lone-pairs and bonding orbital atoms. Additionally, this process was used to estimate the energy of molecules with the same geometry without the need for electronic delocalization. Moreover, it is believed that the E Lewis only applies to electrostatic and static interactions. At high E2 stabilization energies, NBO analysis shows that the only major allowed intermolecular contacts between donor-acceptor electrons are LP-σ* type, whereas at low E2 values, σ-σ* type interactions are presented. On the other hand, the compounds **6a-6d** show no interactions between the π-π* orbitals. The E$^2_{ij}$ of compounds **6a-6d** as second order energy values was compared between donors Lewis-type NBOs and acceptors non-Lewis NBOs and the outcomes are given in Table 8. The energy interaction between σ type bonding orbitals is signified as (BD), lone pair atoms as (LP), the σ* type antibonding orbitals as (BD*) and LP* as E (2). This result displayed intramolecular charge transfer in compounds **6a-6d** where compound **6d** is more than **6a, 6b** and **6c**. The energy contribution for the (C–C) with (C–C) in compounds **6a-6d** is 20.28-30.23 kcal/mol, N with N-C bond is 44.09-70.03 kcal/mol and O with C-O is 35.01-50.19 kcal/mol where the interaction of N with N-C was shown as the largest amount of energy.

Table 8. The NBO analysis of compounds **6a-d**

Compounds	Donor(i)	Type	Acceptor(j)	Type	E(2) kcal/mol
6a	C- C	σ	C - C	π*	20.28
	N	LP	N - C	π*	44.09
	O	LP	C - O	π*	47.56
	S	LP	C - O	π*	24.20
6b	C- C	π*	C - C	π*	21.88
	N	LP	N - C	π*	52.89
	O	LP	C - O	π*	47.01
	S	LP	C - O	π*	20.35
6c	C- C	σ	C - C	π*	21.01
	N	LP	N - C	π*	61.56
	O	LP	C - O	π*	50.19
	S	LP	C - O	π*	21.15
6d	C- C	π*	C - C	π*	30.23
	N	LP	N - C	π*	70.03
	O	LP	C - O	π*	35.01
	S	LP	C - O	π*	43.14

Conclusion
To sum up, this study examined the green and environmentally friendly MCRs of aldehydes, ethyl acetoacetate, urea, or thiourea, electron-deficient acetylenic compounds, tert-butyl isocyanide, and catalytic amounts of Ag/Fe$_3$O$_4$/SiO$_2$@MWCNTs MNCs as effective catalysts in water at room temperature. The results showed that the MNCs produced new derivatives of pyrimidothiazines and pyrimidooxazines with acceptable yields. This investigation also examined the synthesised pyrimidothiazines and pyrimidooxazines **6a–6d** antioxidant activity using two procedures: FRAP and DPPH radical catching, which demonstrated that these compounds had good activity in comparison to conventional antioxidants. Furthermore, we applied the disk diffusion technique to demonstrate the antibacterial activity of synthesized pyrimidothiazines and

pyrimidooxazines against two types of Gram positive and Gram negative bacteria. The outcomes demonstrated that pyrimidothiazines and pyrimidooxazines that were created could stop the growth of bacteria. Among the advantages of these reactions are their high atom economy, high yield product generation, low catalyst quantity, and straightforward reaction.

Data availability statement
The file containing ancillary materials conveys data about prepared compounds that might be helpful for the readers of this article.

Acknowledgments

References
[1] Reymond J-L, Awale M (2012) Exploring chemical space for drug discovery using the chemical universe database. ACS Chem Neurosci 3(9):649-657. doi: 10.1021/cn3000422.

[2] James M J, O'Brien P, Taylor R J K, Unsworth W P (2016) Synthesis of Spirocyclic Indolenines. Chem Eur J 22: 2856. doi: 10.1002/chem.201503835

[3] Welsch ME, Snyder SA, Stockwell BR (2010) Privileged scaffolds for library design and drug discovery. Curr Opin Chem Biol 14: 347-361. doi: 10.1016/j.cbpa.2010.02.018.

[4] Kalaria PN, Karad SC, Raval DK (2018) A review on diverse heterocyclic compounds as the privileged scaffolds in antimalarial drug discovery. Eur J Med Chem 158: 917-936. doi: 10.1016/j.ejmech.2018.08.040.

[5] Desai N, Trivedi A, Pandit U, Dodiya A, Rao VK, Desai P (2016) Hybrid Bioactive Heterocycles as Potential Antimicrobial Agents: A Review. Mini Rev Med Chem 16(18):1500-1526. doi: 10.2174/1389557516666160609075620.

[6] Fouad MM, El-Bendary ER, Suddek GM, Shehata IA, El-Kerdawy MM (2018) Synthesis and in vitro antitumor evaluation of some new thiophenes and thieno[2,3-d]pyrimidine derivatives. Bioorg Chem 81: 587598. doi: 10.1016/j.bioorg.2018.09.022].

[7] Martins P, Jesus J, Santos S, Raposo LR, Roma-Rodrigues C, Baptista PV, Fernandes AR (2015) Heterocyclic Anticancer Compounds: Recent Advances and the Paradigm Shift towards the Use of Nanomedicine's Tool Box. Molecules 20: 16852−16891, doi: 10.3390/molecules200916852.

[8] Siddiqui N, Andalip Bawa S, Ali R, Afzal O, Akhtar MJ, Azad B, Kumar R (2011) Antidepressant potential of nitrogen-containing heterocyclic moieties: An updated review. J Pharm Bioallied Sci 3: 194-212. doi: 10.4103/0975-7406.80765.

[9] Sokolova AS, Yarovaya OI, Bormotov NI, Shishkina LN, Salakhutdinov NF (2018) Synthesis and antiviral activity of camphor-based 1,3-thiazolidin-4-one and thiazole derivatives as Orthopoxvirus-reproduction inhibitors. Med Chem Commun 9:1746-1753. doi:10.1039/C8MD00347E.

[10] Goel A, Agarwal N, Singh FV, Sharon A,Tiwari P, Dixit M, Pratap R, Srivastava AK, Maulik PR, Ram VJ (2004) Antihyperglycemic activity of 2-methyl-3, 4, 5-triaryl-1H-pyrroles in SLM and STZ models. Bioorg Med Chem Lett 14: 1089–1092. doi:10.1016/j.bmcl.2004.01.009.

[11] Amir M, Javed SA, Kumar H (2007) Pyrimidine as antiinflammatory agent: A review. Indian J Pharm Sci 69(3): 337-343. doi: 10.4103/0250-474X.34540.

[12] Li W, Zhao SJ, Gao F, Lv ZS, Tu JY, Xu Z (2018) Synthesis and In Vitro Anti-Tumor, Anti-Mycobacterial and Anti-HIV Activities of Diethylene-Glycol-Tethered Bis-Isatin Derivatives. Chem Select 3:10250–10254. doi:10.1002/slct.201802185.

[13] Zhao X, Chaudhry ST, Mei J (2017) Heterocyclic building blocks for organic semiconductors. Heterocyclic chemistry in the 21st Century a Tribute to Alan Katritzky 121: 133-171.

[14] Khattab TA, Rehan MA (2018 A Review on Synthesis of Nitrogen-Containing Heterocyclic Dyes for Textile Fibers - Part 2: Fused Heterocycles. Egypt J Chem 61: 989–1018. doi:10.21608/ejchem.2018.4131.1363

[15] Lamberth C, Dinges J (2012) Bioactive heterocyclic compound classes: agrochemicals. Wiley-VCH Verlag GmbH & Co, KGaA.

[16] Zhi S, Ma X, Zhang W (2019) Consecutive multicomponent reactions for the synthesis of complex molecules. Org Biomol Chem 17: 7632–7650. doi:10.1039/C9OB00772E.

[17] Ibarra IA, Islas-Jácome A, González-Zamora E (2018) Synthesis of polyheterocycles via multicomponent reactions. Org Biomol Chem 16: 1402–1418. doi:10.1039/C7OB02305G.

[18] Tietze LF, Bsasche C, Gericke KM (2006) Domino reactions in organic synthesis. Wiley-VCH, Weinheim.

[19] Weber L, Illgen K, Almstetter M (1999) Discovery of New Multi Component Reactions with Combinatorial Methods. Synlett 3: 366–374. doi: 10.1055/s-1999-2612.

[20] Herrera RP, Marqués-López E (2015) Multicomponent reactions: concepts and applications for design and synthesis. Wiley, Hoboken.

[21] Sahay R, Sundaramurthy J, Suresh Kumar P, Thavasi V, Mhaisalkar SG, Ramakrishna S (2012) Synthesis and characterization of CuO nanofibers, and investigation for its suitability as blocking layer in ZnO NPs based dye sensitized solar cell and as photocatalyst in organic dye degradation. J Solid State Chem 186: 261-267. doi:10.1016/j.jssc.2011.12.013.

[22] Zhang B-T, Zheng X, Li H-F, Lin J-M (2013) Application of carbon-based nanomaterials in sample preparation: a review. Anal Chim Acta 784:1–17. doi: 10.1016/j.aca.2013.03.054.

[23] Xin T, Ma M, Zhang H, Gu J, Wang S, Liu M, Zhang Q (2014) A facile approach for the synthesis of magnetic separable Fe3O4@TiO2, core–shell nanocomposites as highly recyclable photocatalysts. Appl Surf Sci 288:51–59. doi: 10.1016/j.apsusc.2013.09.108.

[24] Jing J, Li J, Feng J, Li W, Yu WW (2013) Photodegradation of quinoline in water over magnetically separable Fe3O4/TiO2 composite photocatalysts. Chem Eng J 219: 355-360. doi:10.1016/j.cej.2012.12.058

[25] Mandel K, Hutter F, Gellermann C, Sextl G (2013) Reusable superparamagnetic nanocomposite particles for magnetic separation of iron hydroxide precipitates to remove and recover heavy metal ions from aqueous solutions. Sep Purif Technol 109: 144–147. doi: 10.1016/j.seppur.2013.03.002.

[26] Djurišić AB, Chen X, Leung YH, Ching Ng AM (2012) ZnO nanostructures: growth, properties and applications. J Mater Chem 22: 6526-6535. doi:10.1039/C2JM15548F.

[27] (a) Halliwell B (1999). Antioxidant Defence Mechanisms: From the Beginning to the End (of the Beginning). Free Radical Res 31: 261–272, doi:10.1080/10715769900300841. (b) Ahmadi F, Kadivar M, Shahedi M (2007) Antioxidant activity of Kelussia odoratissima Mozaff. in model and food systems. Food Chem 105: 57–64. doi:10.1016/j.foodchem.2007.03.056.

[28] Babizhayev MA, Deyev AI, Yermakovea VN, Brikman IV, Bours J (2004) Lipid peroxidation and cataracts: N-acetylcarnosine as a therapeutic tool to manage age-related cataracts in human and in canine eyes. Drugs in R & D 5:125–39. doi: 10.2165/00126839-200405030-00001.

[29] Liu L, Meydani M (2002) Combined vitamin C and E supplementation retards early progression of arteriosclerosis in heart transplant patients. Nutr Rev 60:368–371. doi: 10.1301/00296640260385810.

[30] A. K. O. Aldulaimi, M. J. Jawad, S. M. Hassan, T. S. Alwan, S. S. S. A. Azziz, Y. M. Bakri,. The potential antibacterial activity of a novel amide derivative against gram-positive and gram-negative bacteria. Int. J. Drug Deliv. Tec., 12(2) (2022) 510-515. doi:10.25258/ijddt.12.2.8

[31] A. K. O. Aldulaimi, A. H. Idan, A. H. Radhi, S. A. Aowda, S. S. S. A. Azziz, W. M. N. H. W. Salleh, A. K. O. Aldulaimi, N. A. M. Ali, Gcms analysis and biological activities of iraq zahdi date palm phoenix dactylifera l volatile compositions. Res. J. Pharm. Tec., 13(11) (2020) 5207-5209. doi:10.5958/0974-360X.2020.00910.5

[32] A. K. O. Aldulaimi, A. A. Majhool, I. S. Hasan, M. Adil, S. M. Saeed, A. H. Adhab New MCRs: Preparation of Novel Derivatives of Pyrazoloazepines in Ionic Liquid and Study of Biological Activity, Polycycl. Aromat. Comp., (2023). DOI: 10.1080/10406638.2023.2254903

[33] S. S. S. A., Azziz, A. K. O. Aldulaimi, S. A. Aowda, Y. M. Bakri, A. A. Majhool, R. M. Ibraheem, F. Abdullah, Secondary metabolites from leaves of polyalthia lateriflora

and their antimicrobial activity. Int. J.Res. Pharm. Sci. 11(3), (2020) 4353-4358. doi:10.26452/ijrps.v11i3.2652

[34] (a) Ezzatzadeh E (2018) Green synthesis of α-aminophosphonates using ZnO-nanoparticles as an efficient catalyst. Zeitschrift für Naturforschung B 73: 179-184, doi:10.1515/znb-2017-0177. (b) Ghanaat, J., Khalilzadeh, M. A., and Zareyee, D. (2020). KF/CP NPs as an efficient nanocatalyst for the synthesis of 1,2,4-triazoles: Study of antioxidant and antimicrobial activity. Eurasian Chem Commun (2), 202-212, doi: 10.33945/SAMI/ECC.2020.2.6 (c) Ezzatzadeh E, Farjam MH, Rustaiyan A (2012) Comparative evaluation of antioxidant and antimicrobial activity of crude extract and secondary metabolites isolated from Artemisia kulbadica. Asian Pac J Trop. Disease 2: S431-S434. doi:10.1016/S2222-1808(12)60198-4. (d) Haddazadeh E, Mohammadi MK (2020) One-pot Synthesize of Phenyl Phenanthro Imidazole Derivatives Catalyzed by Lewis Acid in the Presence of Ammonium Acetate. Chem Methodol 4: 324-332. doi:10.22034/ecc.2021.272326.1136 (e) Mostaghni F, Taat F (2020) CoFe2O4 as green and efficient catalyst for synthesis of multisubstituted imidazoles. Eurasian Chem Commun 2: 427-432. doi.:10.33945/SAMI/ECC.2020.4.1

[35] (a) Hossaini ZS, Zareyee D, Sheikholeslami-Farahani F, Vaseghi S, Zamani A (2017) ZnO-NR as the efficient catalyst for the synthesis of new thiazole and cyclopentadienone phosphonate derivatives in water. Heteroat Chem 28: e21362, doi:10.1002/hc.21362. (b) Sajjadifar S, Amini I, Mansouri G, Alimohammadi S (2020) Fe3O4@APTES@isatin-SO3H as heterogeneous and efficient catalyst for the synthesis of quinoxaline derivatives. Eurasian Chem Commun 2: 626-633. doi:10.33945/SAMI/ECC.2020.5.9. (d) Baghernejad B, Nazari L. (2021) Synthesis of indeno [1,2-b] pyridine derivatives in the precense of Nano CeO2/ZnO. Eurasian Chem Commun3 (5): 319-326. doi:10.22034/ecc.2021.277002.1145. (e) Yavari I, Hossaini ZS, Souri S, Seyfi S (2009) Diastereoselective synthesis of fused [1,3]thiazolo [1,3] oxazins and [1,3] oxazino [2,3-b][1,3] benzothiazoles. Mol Divers 13: 439-443. doi:10.1007/s11030-009-9128-x.

[36] (a) Rustaiyan A, Ezzatzadeh E (2011) Sesquiterpene lactones and penta methoxylated flavone from Artemisia kulbadica. Asian J Chem 23:1774-1776. (b) Khazaei A, Gohari-Ghalil F, Tavasoli M, Rezaei-Gohar M, Moosavi-Zare AR (2020) Fe3O4 Bonded Pyridinium-3-carboxylic acid-N-sulfonic Acid Chloride as an Efficient Catalyst for the Synthesis of 3,4-dihydropyrimidin-2(1H)-ones. Chem Methodol 4: 543-553. doi:10.22034/chemm.2020.106433. (c) Taran J, Ramazani A, Atrak K (2020) Silica nanoparticles as highly efficient catalyst for the one-pot synthesis of α-aminophosphonate derivatives from primary amines, quinoline-4-carbaldehyde and phosphite under solvent-free conditions . Eurasian Chem Commun 2: 257-264. doi:10.33945/SAMI/ECC.2020.2.11. (d) Baghernejad B, Rostami Harzevili M (2021) Nano-cerium

Oxide/Aluminum Oxide: An Efficient and Useful Catalyst for the Synthesis of Tetrahydro[a]xanthenes-11-one Derivatives Chem Methodol 5 2: 90-95. doi:10.22034/chemm.2021.119641. (e) Rajabi M, Hossaini ZS, Khalilzadeh MA, Datta Sh, Halder M, Mousa SA (2015) Synthesis of a New Class of Furo[3,2-C]Coumarins and its Anticancer Activity. J Photochem Photobio B: Biol 148: 66-72. doi:10.1016/j.jphotobiol.2015.03.027.

[37] (a) Rostami-Charati F, Hossaini ZS, Rostamian R, Zamani A, Abdoli M (2017) Green synthesis of indol-2-one derivatives from N-alkylisatins in the presence of KF/clinoptilolite nanoparticles. Chem Heterocyl Comp. 53: 480-483. doi:10.1007/s10593-017-2077-x. (b) Ghanaat J, Khalilzadeh MA, Zareyee D (2020) KF/CP NPs as an efficient nanocatalyst for the synthesis of 1,2,4-triazoles: Study of antioxidant and antimicrobial activity. Eurasian Chem Commun 2: 202-212, doi: 10.33945/SAMI/ECC.2020.2.6. (c) Rezayati S, Sheikholeslami-Farahani F, Hossaini ZS, Hajinasiri R, Afshari Sharif Abad S (2016) Regioselctive thiocyanation of aromatic and heteroaromatic compounds using a novel bronsted acidic ionic liquid. Comb Chem High Throughput Screen 9: 720-727.doi: 10.2174/1386207319666160709191851. (d) Seifi Mansour S, Ezzatzadeh E, Safarkar R (2019) In vitro evaluation of its antimicrobial effect

of the synthesized Fe3O4 nanoparticles using Persea Americana extract as a green approach on two standard strains. Asian J Green Chem 3: 353-365. https://doi.org/10.22034/ajgc.2018.154682.1113. (e) Haddazadeh E, Mohammadi MK (2020) One-pot Synthesize of Phenyl Phenanthro Imidazole Derivatives Catalyzed by Lewis Acid in the Presence of Ammonium Acetate. Chem Methodol 4: 324-332. doi:10.22034/ecc.2021.272326.1136. (f) Al-Haidari AS, Al-Tamimi EO (2021) Synthesis of new derivatives of 1,3,4-thiadiazole and 1,3,4-oxadiazole on cyclic imides and studying their antioxidant. Eurasian Chem Commun 3: 508-517. http://dx.doi.org/10.22034/ecc.2021.289788.1185.

[38] (a) Rostami Charati F, Hossaini ZS, Hosseini-Tabatabaei MR (2011) A simple synthesis of oxaphospholes. Phosphorus Sulfur Silicon Relat Elem 186: 1443-1448. doi:10.1080/10426507.2010.515953. (b) Sajjadi-Ghotbabadi H, Javanshir SH, Rostami-Charati F (2016) Nano KF/Clinoptilolite: An Effective Heterogeneous Base Nanocatalyst for Synthesis of Substituted Quinolines in Water. Catal Lett 146: 338–344. doi:10.1007/s10562-015-1652-y. (c) Aghahosseini H, Ramazani A (2020) Magnetite L-proline as a reusable nano-biocatalyst for efficient synthesis of 4H-benzo[b]pyrans in water: a green protocol. Eurasian Chem Commun 2: 410-419, doi:10.33945/SAMI/ECC.2020.3.11. (d) Yavari I, Hossaini ZS, Souri S, Seyfi S (2009) Diastereoselective synthesis of fused [1,3] thiazolo [1,3] oxazins and [1,3] oxazino [2,3-b][1,3] benzothiazoles. Mol Divers 13:439-443. doi:10.1007/s11030-009-9128-x. (e) Yavari I,

Nematpour M, Hossaini ZS (2010). Ph3P-mediated one-pot synthesis of functionalized 3, 4-dihydro-2H-1, 3-thiazines from N, N′-dialkylthioureas and activated acetylenes in water. Monatsh fur Chem 141: 229-232. doi:10.1007/s00706-009-0247-y. (f) Karimi AH, Hekmat-Ara A, Zare A, Barzegar M, Khanivar R, Sadeghi-Takallo M (2021) Producing, characterizing and utilizing a novel magnetic catalyst to promote construction of N,N′-alkylidene bisamides. Eurasian Chem Commun 3: 360-38. doi:10.22034/ecc.2021.277415.1149 .

[39] (a) Hajinasiri R, Hossaini ZS, Rostami-Charati F (2011) Efficient synthesis of α-aminophosphonates via one-pot reactions of aldehydes, amines, and phosphates in ionic liquid. Heteroat Chem 22: 625-629, doi.org/10.1002/hc.20724. (b) Nikpassand M, Zare Fekri L (2020) Catalyst-free Synthesis of Mono and Bis Spiro Pyrazolopyridines in DSDABCO as a Novel Media. Chem Methodol 4: 437-332. doi:10.33945/SAMI/CHEMM.2020.4.6. (c) Ezzatzadeh E, Sofla SFI, Pourghasem E, Rustaiyan A, Zarezadeh A (2014) Antimicrobial Activity and Chemical Constituents of the Essential Oils from Root, Leaf and Aerial Part of Nepeta asterotricha from Iran. J. Essent. Oil-Bear. Plants 17: 415-421. https://doi.org/10.1080/0972060X.2014.901624. (d) Ahmadi N, Ramazani A, Rezayati S, Hosseini F (2020) Synthesis of silica nanoparticles and study of its catalytic properties in the preparation of carboxylic esters. Eurasian Chem Commun 2: 862-874. doi:10.22034/ecc.2020.108366. (e) Rustaiyan A, Masoudi S, Ezzatzadeh E, Akhlaghi H, Aboli J. Composition of the Aerial Part, Flower, Leaf and Stem Oils of Eremostachys macrophylla Montbr. & Auch. and Eremostachys labiosa Bunge. from Iran. J. Essent. Oil-Bear. Plants 14 (2011): 84-88. https://doi.org/10.1080/0972060X.2011.10643904.

[40] (a) Mostaghni F, Taat F (2020) CoFe2O4 as green and efficient catalyst for synthesis of multisubstituted imidazoles Eurasian Chem. Commun. 2: 427-432. doi:10.33945/SAMI/ECC.2020.4.1 (b) Rezayati S, Hajinasiri R, Hossaini ZS, Abbaspour S (2018) Chemoselective synthesis of 1,1-diacetates (acylals) using 1,1'- butylenebispyridinium hydrogen sulfate as a new, halogen-free and environmental-friendly catalyst under solvent-free

conditions. Asian J Green Chem 2: 268-280. doi: 10.22034/ajgc.2018.61810. (c) Raoufi F, Aghaei H, Ghaedi M (2020) Cu-metformin grafted on multi walled carbon nanotubes: Preparation and investigation of catalytic activity. Eurasian Chem Commun 2: 226-233.doi:10.33945/SAMI/ECC.2020.2.8. (d) Salih AR, Al-Messri ZAK (2021) Synthesis of pyranopyrazole and pyranopyrimidine derivatives using magnesium oxide nanoparticles and evaluation as corrosion inhibitors for lubricants. Eurasian Chem Commun 3: 533-541. doi:10.22034/ecc.2021.291144.1189.

[41] (a) Hamedani NF, Zamani Hargalani F, Rostami- Charati F (2021) Biosynthesis of Cu/KF/Clinoptilolite@ MWCNTs nanocomposite and its application as a recyclable nanocatalyst for the synthesis of new Schiff base of benzoxazine derivatives and reduction of organic pollutants. Mol Divers 26(4):2069-2083. doi: 10.1007/s11030-021-10316-1. (b) Hakimi F, Fallah-Mehrjardi M, Golrasan E (2020) Yttrium Aluminum Garnet (YAG: Al5Y3O12) as an Efficient Catalyst for the Synthesis of Benzimidazole and Benzoxazole Derivatives. Chem Methodol 4: 234-244, doi:10.33945/SAMI/CHEMM/2020.3.2. (c) Ezzatzadeh E (2021) Chemoselective oxidation of sulfides to sulfoxides using a novel Zn-DABCO functionalized Fe3O4 MNPs as highly effective nanomagnetic catalyst, Asian J Nanosci Mater 4: 125-136. DOI: 10.26655/AJNANOMAT.2021.2.3. (d) Kamali F, Shirini F (2021) Effective and convenient synthesis of 2-amino-4H-chromenes promoted by melamine as a recyclable organocatalyst. Eurasian Chem Commun 3: 278-290. doi:10.22034/ecc.2021.272326.1136. (e) Mohammed Abd Al-Mohson Z, (2021) Synthesis of novel pyrazole derivatives containing tetrahydrocarbazole, antimicrobail evaluation and molecular properties. Eurasian Chem Commun 3: 425-434. doi:10.22034/ecc.2021.284257.1173Z.

[42] (a) Baghernejad B, Fiuzat M (2020) A new strategy for the synthesis of 2-amino-4H-pyran derivatives in aqueous media using DABCO-Cucl complex as a novel and efficient catalyst. Eurasian Chem Commun 2 (11): 1088-1092.http://dx.doi.org/10.22034/ecc.2020.250740.1078. (b) Albadi J, Samimi HA, Momeni AR (2020) Alumina-Supported Cobalt Nanoparticles Efficiently Catalyzed the Synthesis of Chromene Derivatives under Solvent-Free Condition. Chem Methodol 4:565-571. https://doi.org/10.22034/chemm.2020.107071. (c) Ebrahimi Z, Davoodnia A, Motavalizadehkakhky A, Mehrzad J (2020) Synthesis, characterization, and molecular structure investigation of new tetrahydrobenzo[b]thiophene-based Schiff bases: A combined experimental and theoretical study. Eurasian Chem Commun 2: 170-180. doi:10.33945/SAMI/ECC.2020.2.2. (d) Dehghani N, Babamoradi M, Hajizadeh Z, Maleki A (2020) Improvement of Magnetic Property of CMC/Fe3O4 Nanocomposite by Applying External Magnetic Field During Synthesis. Chem Methodol 4:92-99. (e) Tayebee R, Gohari A (2020) The dual role of ammonium acetate as reagent and catalyst in the synthesis of 2, 4, 5-triaryl-1H-imidazoles. Eurasian Chem Commun 2: 581-586. doi:10.33945/SAMI/ECC.2020.5.3R.

[43] Ahmed Kareem Obaid Aldulaimi; Ali H. Hussein; Moayad Jasim Mohammed; Haider Radhi Saud; Hala Bashir; Farinaz Shahimi, hydroxyazidation of alkenes: A viable strategy for the synthesis of β-azido alcohols, Chem. Rev. Lett. 7 (2024) 10.22034/crl.2024.430494.1270.

[44] Ahmed Kareem Obaid Aldulaimi; Moayad Jasim Mohammed; Saad Khudhur Mohammed; Hala Bashir; Ayat A. Hussein; Farnaz Behmagham, Recent Progress on 1,2-Hydroxyfluorination of Alkenes, Chem. Rev. Lett. 7 (2024). 10.22034/crl.2024.428584.1264

[45] Alhussein Arkan Majhool; Mohanad Yakdhan Saleh; Ahmed Kareem Obaid Aldulaimi; Shakir Mahmood Saeed; Saif M. Hassan; Mohamed F. El-Shehry; Samir Mohamed Awad; Saripah Salbiah Syed Abdul Azziz, Synthesis of New Azo Dyes of Uracil via Ecofriendly Method and Evaluation For The Breast, Liver and Lung Cancer Cells In vitro, Chem. Rev. Lett. 6 2023) 442-448. 10.22034/crl.2023.425031.1258

[46] A. K. O. Aldulaim, N. M. Hameed, T. A. Hamza, A. S. Abed, The antibacterial characteristics of fluorescent carbon nanoparticles modified silicone denture soft liner. J. Nanostruct., 12 (2022) 774-781. doi:10.22052/JNS.2022.04.001

[47] Rajendran SP, Sengodan K (2017) Synthesis and Characterization of Zinc Oxide and Iron Oxide Nanoparticles Using Sesbania grandiflora Leaf Extract as Reducing Agent. J. Nanoscience 17: 1-7. doi:10.1155/2017/8348507.

[48] Shimada K, Fujikawa K, Yahara K, Nakamura T (1992) Antioxidative properties of xanthan on the autoxidation of soybean oil in cyclodextrin emulsion. J Agric Food Chem 40: 945–948. doi: 10.1021/jf00018a005.

[49] Yen G C, Duh P D (1994) Scavenging Effect of Methanolic Extracts of Peanut Hulls on Free-Radical and Active-Oxygen Species. J Agric Food Chem 42: 629–32, doi: 10.1021/jf00039a005.

[50] Yildirim A, Mavi A, Kara AA (2001). Determination of antioxidant and antimicrobial activities of Rumex crispus L. extracts. J Agric Food Chem 49: 4083-4089. doi: 10.1021/jf0103572.

[51] Frisch MJ, Trucks GW, Schlegel H B, Scuseria G E, Robb M A, Cheeseman JR, et al. (2009). Gaussian 09 (revision A.02). Wallingford, CT: Gaussian.

[52] Becke AD (1993) Density-functional thermochemistry. III. The role of exact exchange. J Chem Phys 98: 5648. doi:10.1063/1.464913

[53] Lee C, Yang W, Parr RG (1988) Development of the Colle-Salvetti correlation-energy formula into a functional of the electron density. Phys Rev B Condens Matter 37:785-789. doi: 10.1103/physrevb.37.785

[54] Umadevi P, Lalitha P (2012) Synthesis and Antimicrobial Evaluation of Imino Substituted 1, 3, 4 Oxa and Thiadiazoles. Int J Pharm Pharm Sci 4: 523-527.

[55] Lu T, Chen F (2012) Multiwfn: A multifunctional wavefunction analyzer. J Comput Chem 33: 580-592. doi:10.1002/jcc.22885.

[56] Saundane AR, Nandibeoor MK (2015) Synthesis, characterization, and biological evaluation of Schiff bases containing indole moiety and their derivatives. Monatshefte für Chemie - Chemical Monthly 146: 1751-1761, doi:10.1007/s00706-015-1440-9.

[57] Bidchol AM, Wilfred A, Abhijna P, Harish R (2011) Free Radical Scavenging Activity of Aqueous and

Ethanolic Extract of Brassica oleracea L. var. italic. Food and Bioprocess Tech 4: 1137-1143, doi: 10.1007/s11947-009-0196-9.

[58] Mulliken RS (1995) Electronic Population Analysis on LCAO–MO Molecular Wave Functions. J Chem Phys23:1833. doi:10.1063/1.1740588.

[59] Venkatesh G, Govindaraju M, Vennila P, Kamal C (2016) Molecular structure, vibrational spectral assignments (FT-IR and FT-RAMAN), NMR, NBO, HOMO–LUMO and NLO properties of 2-nitroacetophenone based on DFT calculations. J Theoretical & Computational Chem 15(1):1650007. doi:10.1142/S0219633616500073.

[60] Mebi AC (2011) DFT study on structure, electronic properties, and reactivity of cis-isomers of [(NC 5 H 4 –S) 2 Fe(CO)2]. J Chem Sci 123: 727-731. doi:10.1007/s12039-011-0131-2.

[61] Muthu S, Prasath M, Paulraj EI, Balaji RA (2014) FT-IR, FT-Raman spectra and ab initio HF and DFT calculations of 7-chloro-5-(2-chlorophenyl)-3-hydroxy-2,3-dihydro-1H-1,4-benzodiazepin-2-one. Spectroc. Acta A. Mol Biomol Spectrosc 120: 185-194. doi: 10.1016/j.saa.2013.09.150.